

Citation for published version:

Haouari, C, Squires, AG, Berthelot, R, Stievano, L, Sougrati, MT, Morgan, BJ, Lebedev, OI, Iadecola, A, Borkiewicz, OJ & Dambournet, D 2021, 'Impact of Solution Chemistry on Growth and Structural Features of Mo-Substituted Spinel Iron Oxides', *Inorganic Chemistry*, vol. 60, no. 10, pp. 7217-7227.
<https://doi.org/10.1021/acs.inorgchem.1c00278>

DOI:

[10.1021/acs.inorgchem.1c00278](https://doi.org/10.1021/acs.inorgchem.1c00278)

Publication date:

2021

Document Version

Peer reviewed version

[Link to publication](#)

This document is the Accepted Manuscript version of a Published Work that appeared in final form in *Inorg. Chem*, copyright © American Chemical Society after peer review and technical editing by the publisher. To access the final edited and published work see <https://pubs.acs.org/doi/10.1021/acs.inorgchem.1c00278>

University of Bath

Alternative formats

If you require this document in an alternative format, please contact:
openaccess@bath.ac.uk

General rights

Copyright and moral rights for the publications made accessible in the public portal are retained by the authors and/or other copyright owners and it is a condition of accessing publications that users recognise and abide by the legal requirements associated with these rights.

Take down policy

If you believe that this document breaches copyright please contact us providing details, and we will remove access to the work immediately and investigate your claim.

Supplementary Information

The Impact of Solution Chemistry on Growth and Structural Features of Mo-substituted Spinel Iron Oxides

Chérazade Haouari^{a,b,c}, Alexander G. Squires^{d,e}, Romain Berthelot^{a,c*}, Lorenzo Stievano^{a,c*}, Moulay Tahar Sougrati^{a,c}, Benjamin J. Morgan^{d,e}, Oleg I. Lebedev^f, Antonella Iadecola^c, Olaf J. Borkiewicz^g, Damien Dambournet^{b,c*}

^a ICGM, Univ. Montpellier, ENSCM, CNRS, Montpellier, France

^b Sorbonne Université, CNRS, Physico-chimie des électrolytes et nano-systèmes interfaciaux, PHENIX, F-75005 Paris, France

^c Réseau sur le Stockage Electrochimique de l'Energie (RS2E), CNRS, Amiens, France

^d Department of Chemistry, University of Bath, BA2 7AY Bath, United Kingdom

^e The Faraday Institution, Quad One, Harwell Science and Innovation Campus, Didcot OX11 0RA, U.K

^f Laboratoire CRISMAT, ENSICAEN, Université de Caen, CNRS, F-14050, Caen, France

^g X-ray Science Division, Advanced Photon Source, Argonne National Laboratory, 9700 South Cass Avenue, Argonne, Illinois 60439, United States

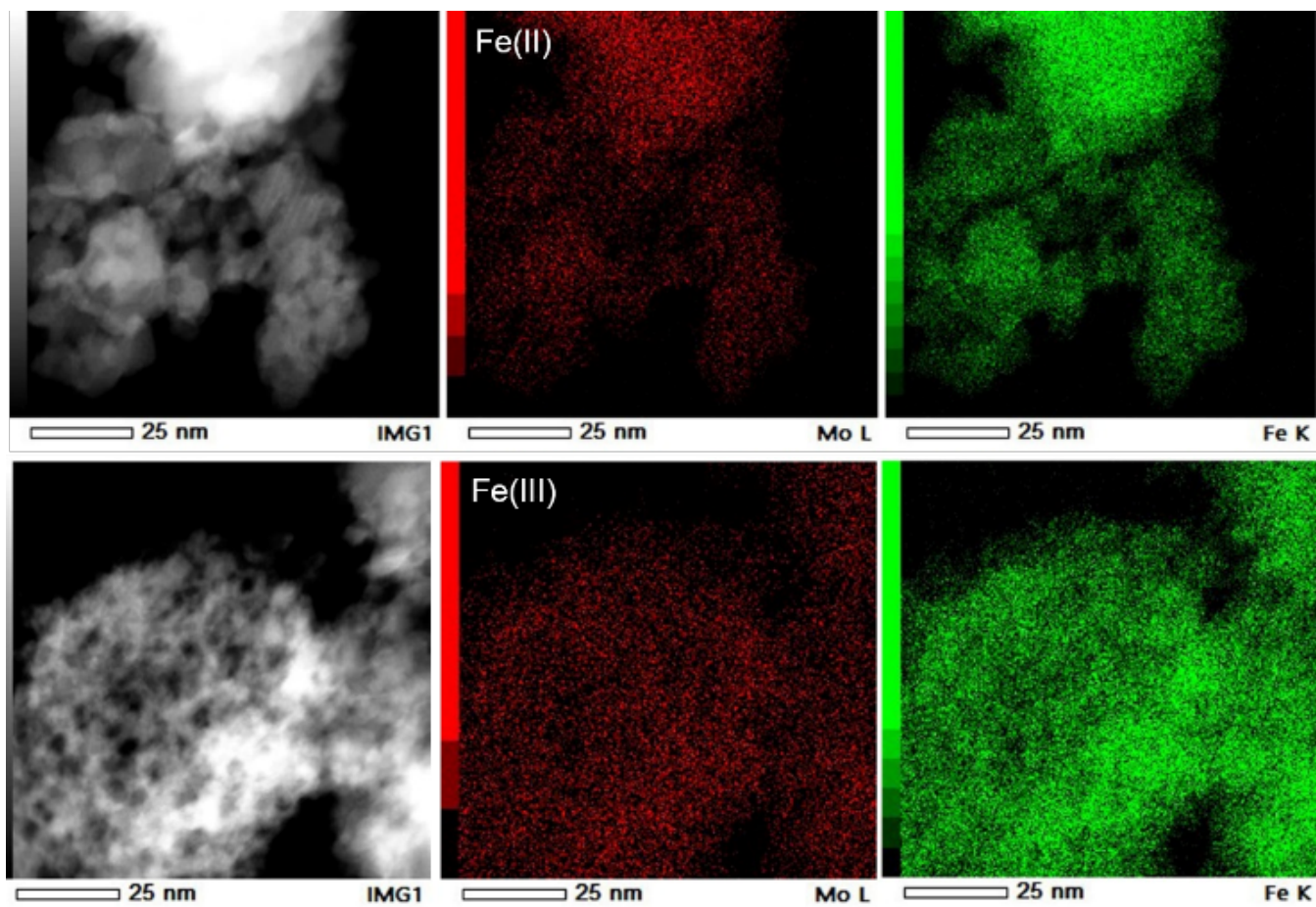


Figure S1. HAADF-STEM images of an isolated particle and corresponding EDX elemental mapping for Mo L and Fe K on the samples prepared with Fe(II) and Fe(III) precursors.

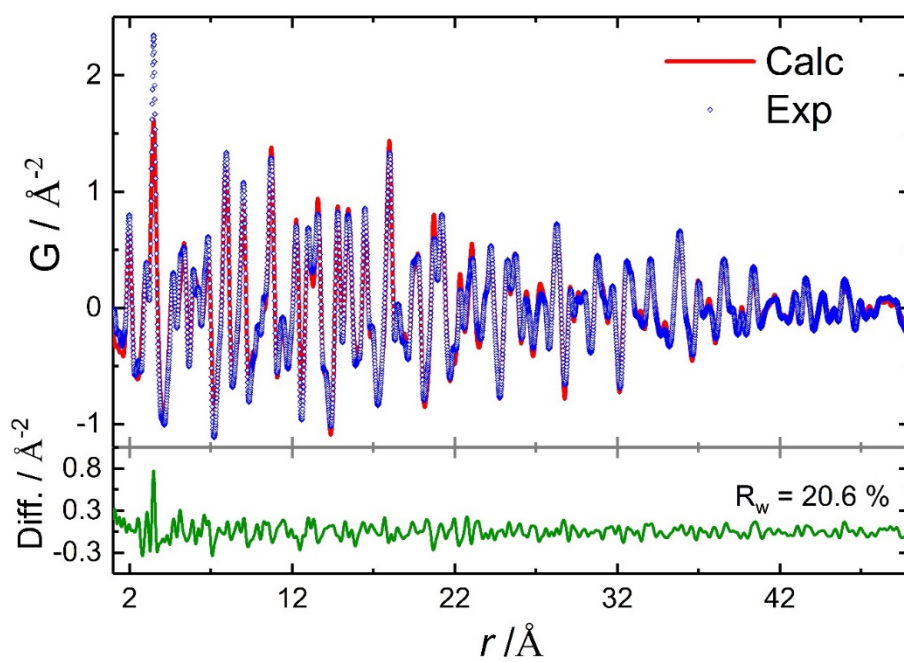


Figure S2. Refinement of the PDF data of the sample prepared with Fe(II) using a two-phase model based on $Fd-3m$ and $P4_32$ space groups.

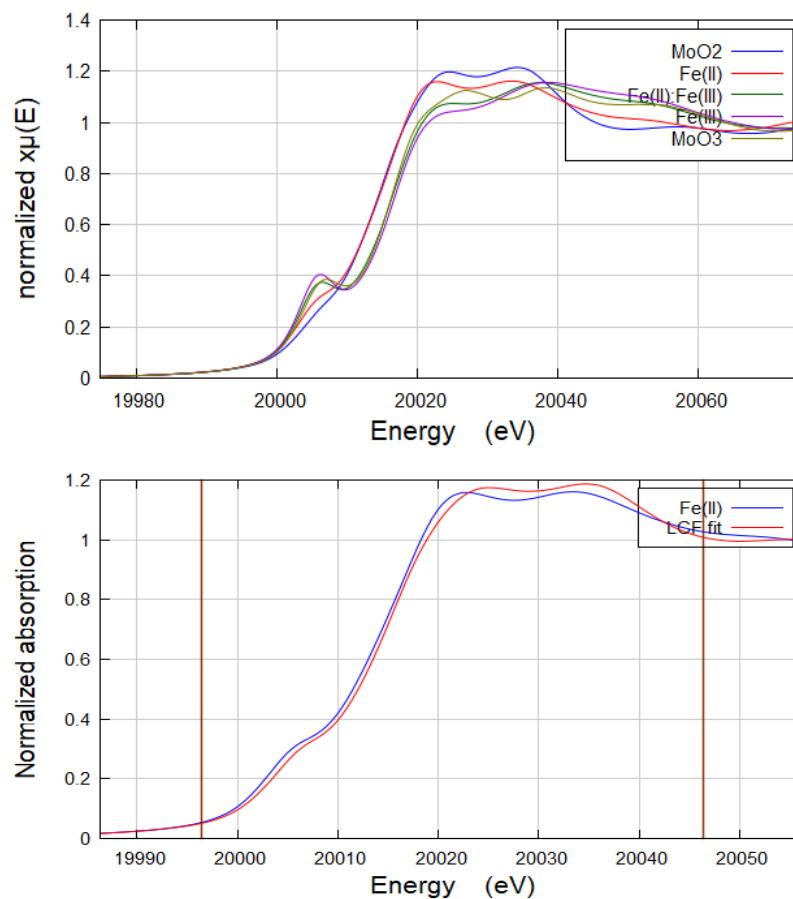


Figure S3. Top: comparison of the XANES signatures of the three samples obtained with different Fe precursors with the experimental spectra of MoO₂ and MoO₃ references. Bottom: linear combination fit of the XANES spectrum of the sample obtained starting from Fe(II) carried out using the spectra of MoO₂ and MoO₃ as references for Mo(IV) and Mo(VI), respectively, which provides a Mo(IV)/Mo(VI) ratio of content of about 3.

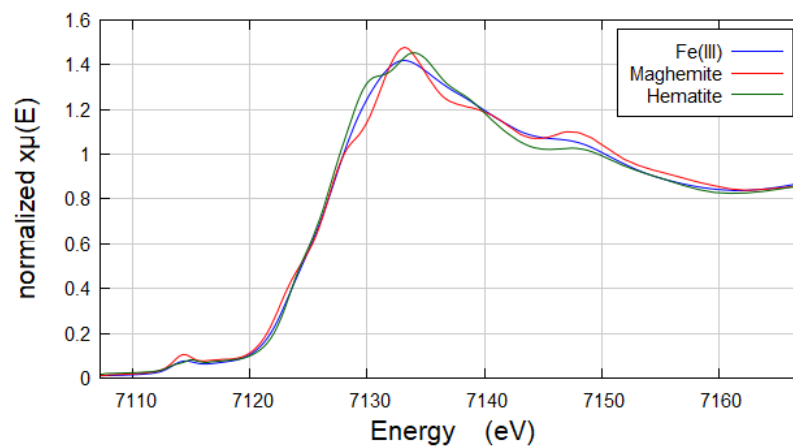


Figure S4. Comparison of the XANES signatures of the sample obtained with the Fe(III) precursor with the experimental spectra of hematite and maghemite references.

Mo and Fe K-edge XAS fitting procedure

The two series of spectra were fitted in the R space in the range 1.0-3.5 Å using the following approach for both Mo and Fe K-edge spectra:

- The first shell, between 1 and 2 Å, was divided in two contributions. The first contributions, including 4 oxygen neighbors, was set at a distance of about 1.8 Å, whereas the second one, including 6 oxygen neighbors, was set at a distance of 2.0 Å. The sum of the relative intensities of the two contributions was set equal to the value of the amplitude factor S_0^2 , which was previously determined to be 0.8 and 0.75 for the Mo and Fe K-edge spectra by fitting the experimental spectrum of a reference material (crystalline MoO_3 and $\alpha\text{-Fe}_2\text{O}_3$, respectively) measured in the same conditions. The σ^2 Debye-Waller factor was fitted to an identical value for both contributions.
- The second shell, between 2 and 3.5 Å was fitted in a simplified manner considering only the contributions of two Fe neighbors at different distances. Considering that, in the theoretical spectrum of spinels, octahedral iron centers are surrounded by 6 Fe neighbors at about 3 Å and 6 more at 3.45 Å, whereas tetrahedral iron centers are only surrounded by 12 neighbors at 3.45 Å, the relative intensity of the first contribution was set equal to that of octahedral Fe-O₄ sites, and that of the second contribution to the weighted average between the intensities of octahedral and tetrahedral first-shell Fe-O_n sites. The σ^2 Debye-Waller factor was fitted to an identical value for both contributions.

The results of the fittings are shown in Figure S5 and S6, and the corresponding fitting parameters reported in Tables S1 and S2 for the Mo and Fe K-edges, respectively.

Sample precursors	Site	S₀²	%	R / Å	σ²
Fe(II)	Mo-O ₄	0.31(4)	39(5)	1.72(3)	0.003(2)
	Mo-O ₆	0.49(4)	61(5)	1.99(3)	
	Mo-Fe ₆	0.49(4)	-	3.14(4)	0.006(2)
	Mo-Fe ₁₂	0.4(1)	-	3.46(4)	
Fe(II):Fe(III)	Mo-O ₄	0.68(6)	85(8)	1.74(4)	0.005(3)
	Mo-O ₆	0.12(6)	15(8)	2.03(4)	
	Mo-Fe ₆	0.12(6)	-	3.17(7)	0.006(5)
	Mo-Fe ₁₂	0.07(5)	-	3.51(7)	
Fe(III)	Mo-O ₄	0.77(2)	95(3)	1.75(1)	0.005(3)
	Mo-O ₆	0.03(2)	5(3)	2.05(3)	
	Mo-Fe ₆	0.03(2)	-	2.82(5)	0.006(5)
	Mo-Fe ₁₂	0.02(2)	-	3.3(1)	

Table S1. Fitting parameters obtained by refining the Mo K-edge EXAFS spectra of the samples prepared using different iron precursors.

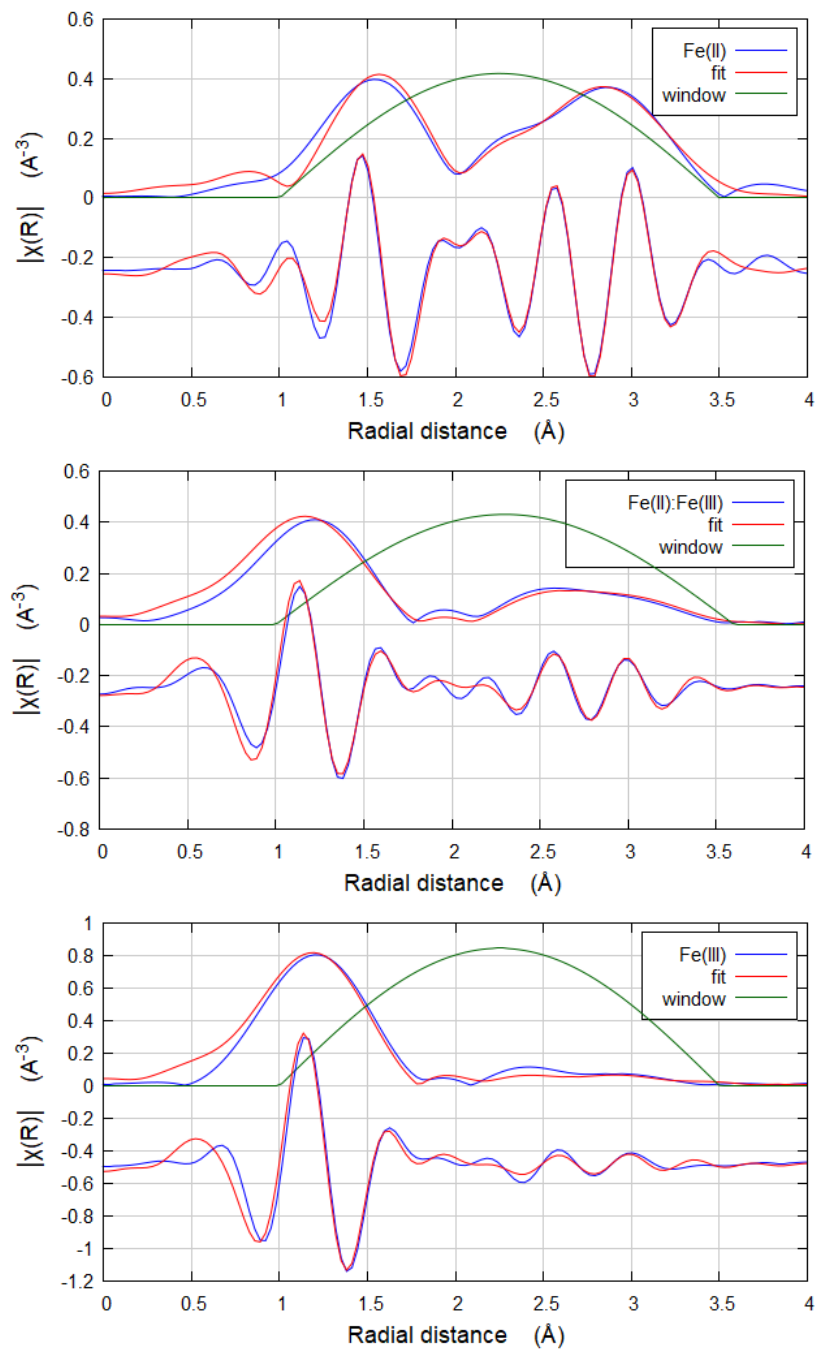


Figure S5. Fits of the Mo K-edge EXAFS spectra of the samples prepared using different iron precursors (left).

Sample precursors	Site	S_0^2	%	R / Å	σ^2
Fe(II)	Fe-O ₄	0.37(7)	49(9)	1.89(2)	0.008(2)
	Fe-O ₆	0.38(7)	51(9)	1.99(2)	
	Fe-Fe ₆	0.38(8)	-	2.98(2)	0.012(3)
	Fe-Fe ₁₂	0.56(8)	-	3.44(2)	
Fe(II):Fe(III)	Fe-O ₄	0.33(6)	44(8)	1.89(3)	0.007(2)
	Fe-O ₆	0.42(6)	56(8)	1.97(2)	
	Fe-Fe ₆	0.42(6)	-	2.99(2)	0.015(3)
	Fe-Fe ₁₂	0.53(6)	-	3.41(3)	
Fe(III)	Fe-O ₄	0.23(7)	34(9)	1.89(3)	0.008(2)
	Fe-O ₆	0.52(7)	66(9)	1.96(2)	
	Fe-Fe ₆	0.52(7)	-	3.02(2)	0.018(3)
	Fe-Fe ₁₂	0.49(7)	-	3.39(3)	

Table S2. Fitting parameters obtained by refining the Fe K-edge EXAFS spectra of the samples prepared using different iron precursors.

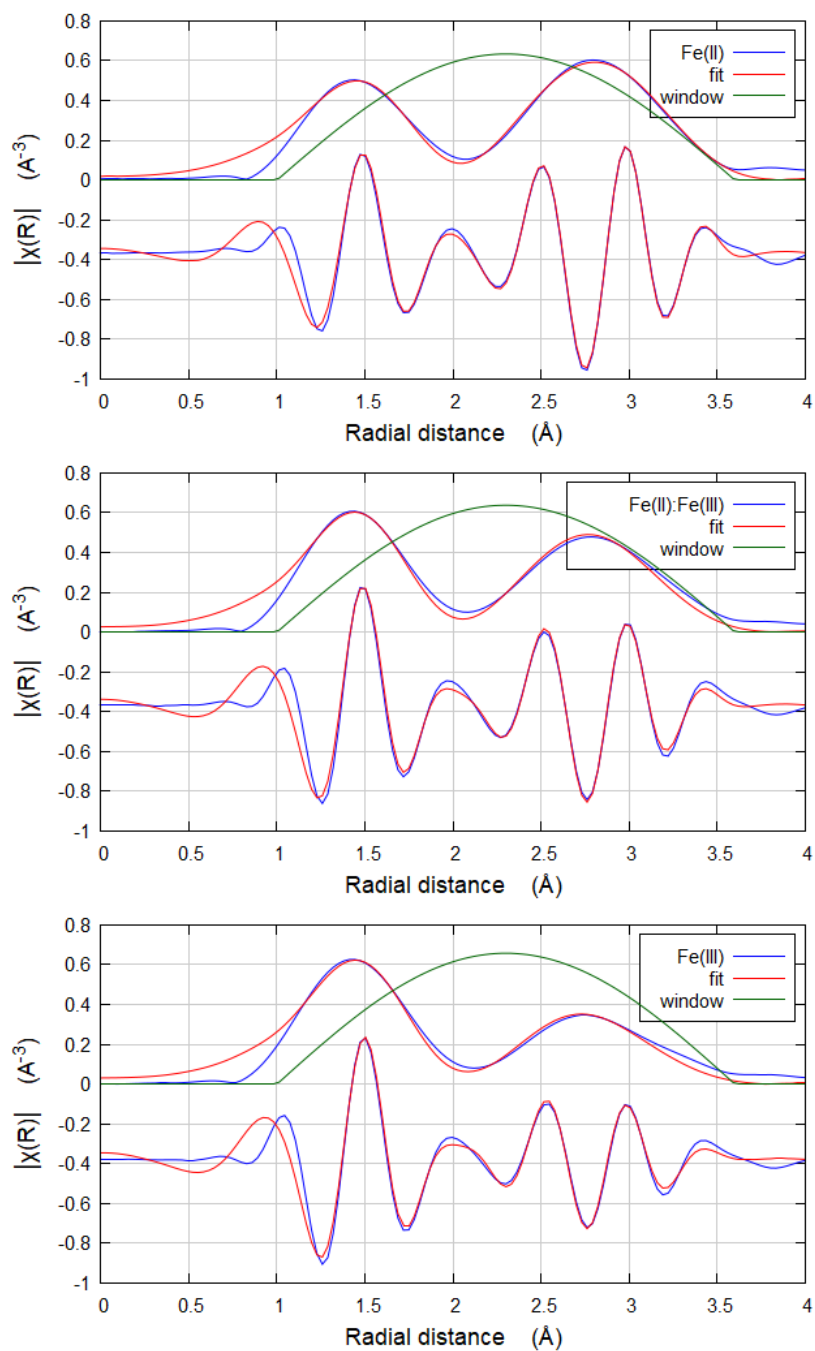


Figure S6. Fits of the Fe K-edge EXAFS spectra of the samples prepared using different iron precursors.

Sample precursors	Site	B_{hf} (T)	Δ (mm/s)	δ (mm/s)	Area (%)
Fe(II)	Fe(III)	-	0.62(2)	0.33(1)	15(2)
	Fe ^{2.5+} sextet	40(1)	0.00	0.88(2)	20(2)
	Fe(III) distr.	30-48	0.00	0.35(2)	65(3)
Fe(II):Fe(III)	Fe(III) T _d	-	0.48(5)	0.25(1)	16(2)
	Fe(III) O _h	-	0.65(4)	0.33(2)	15(3)
	Fe(III) distr.	30-48	0.00	0.33(1)	69(3)
Fe(III)	Fe(III)	-	0.68(1)	0.34(1)	100

Table S3. ⁵⁷Fe hyperfine parameters obtained by fitting the ⁵⁷Fe Mössbauer spectra at room temperature of the samples prepared using different iron precursors.

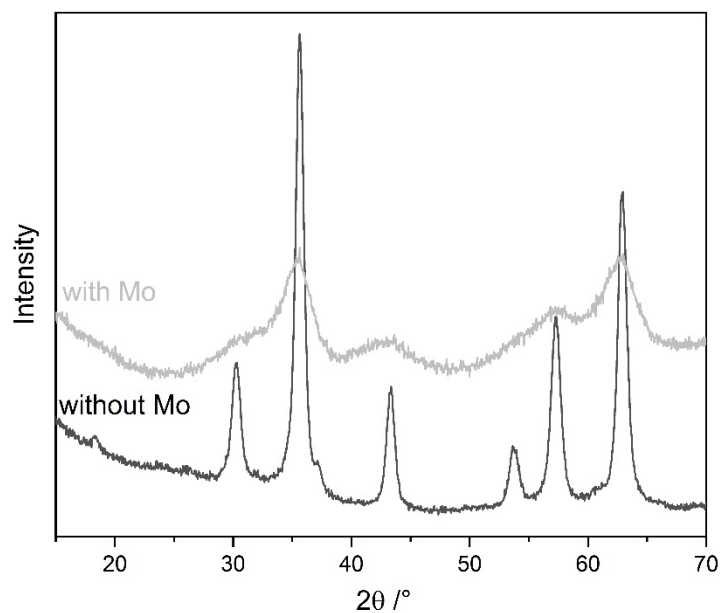


Figure S7. XRD patterns of the samples prepared with and without Mo. The samples were synthesized using an equimolar ratio of Fe(II) and Fe(III).